Journal of Applied Mechanics and Technical Physics, Vol. 36, No. 2, 1995

NUMERICAL INVESTIGATION OF SUPERSONIC TURBULENT SEPARATED FLOWS IN THE VICINITY OF OBLIQUE STEPS

A. V. Borisov, A. A. Zheltovodov, D. Badekas, and N. Narayanswami

UDC 532.526

Prediction of the properties of turbulent separated flows is among the most complicated and pressing problems of fluid mechanics. The lack of a unified and reliable theoretical basis for their analysis impedes the development of computation methods. In this connection present-day computation models call for the use of experimental data. It has been possible to describe some properties of turbulent separation within the limits of ideal gas behavior [1-4]. The approaches that were based on the application of kinetically consistent difference schemes turned out to be efficient in a number of cases [5]. The development of integral and numerical methods derived from equations for a turbulent boundary layer extended the possibilities of solving applied problems considerably and also made it possible to refine many physical properties discovered in experiments [6-8]. Finally, the improvement of numerical methods for solving the averaged Navier–Stokes equations, which make it possible to obtain detailed information on the different flows under consideration [9-11], is natural and promising. The development of all the above-mentioned lines of inquiry depends to a large measure on information supplied by the experimental investigations which are used for the construction of physical models, the justification of closure relationships (of turbulence models), and the testing of computation procedures as well.

The use of the averaged Navier–Stokes equations in solving applied problems requires the development of effective algorithms and the justification of reliable turbulence models. The effectiveness of an algorithm is defined first of all by its efficiency and accuracy. The procedure efficiency depends mainly on the stability of the scheme being used (severity of restriction on a time interval) and the possibility of its stepwise implementation by the simplest procedures (scalar runs) [12]. As a rule, a choice of a turbulence model is justified by the adequacy of the description of characteristic physical processes, mathematical simplicity, and compatibility with the numerical methods employed [13].

The experience gained thus far testifies that the differential models of turbulence with two equations for determining characteristic length and velocity scales are most effective in calculating separated flows. Among them are the well-known models of the $k - \varepsilon$ [14], $q - \omega$ [15], $k - \omega^2$ [16], etc., types. Such models enable one to predict the characteristics of the flows under consideration, including friction and heat-transfer changes in the vicinity of separation zones, more accurately than simpler algebraic ones. At the same time their use calls for additional information on turbulence characteristics to specify the initial conditions which ensure the stability of a computation procedure, especially in the initial stage. Usually, this problem is solved by obtaining numerically calculated parameters for the boundary layer, which develops ahead of interaction zones, or defining the initial airfoils substantiated by reliable experiments. In many instances it is precisely a poor choice of the starting distributions of turbulence characteristics that brings about computation instability.

A fairly large number of numerical investigations are devoted to analysis of interactions of the turbulence boundary layer with incident shock waves or the ones generated in a flow past compression corners [17-21]. Flows that are characterized by interaction of the boundary layer with a sequence of different disturbances, for instance, shock and expansion waves, are widely encountered in practice. Their main feature is the possibility of manifestation of relaxation (hereditary) properties, which are attributed to the preceding disturbance in the zone of a subsequent one, in the boundary layer. Such mixed interactions take place, for instance, in a supersonic flow past oblique-side steps or ledges and apparently represent extreme cases for testing numerical computations and turbulence models. The results of detailed experimental investigations into these configurations are presented in [22-25]. They were used to test the parabolized [26] and complete [10, 27-31] two-dimensional Navier–Stokes equations averaged according to Favre and supplemented by different algebraic and differential models of turbulence.

Institute of Theoretical and Applied Mechanics, Siberian Division of the Russian Academy of Sciences, Novosibirsk 630090. Rutgers University, New Jersey. Translated from Prikladnaya Mekhanika i Tekhnicheskaya Fizika, No. 2, pp. 68-80, March-April, 1995. Original article submitted April 2, 1994.

 0021-8944/95/3602-0210$12.50

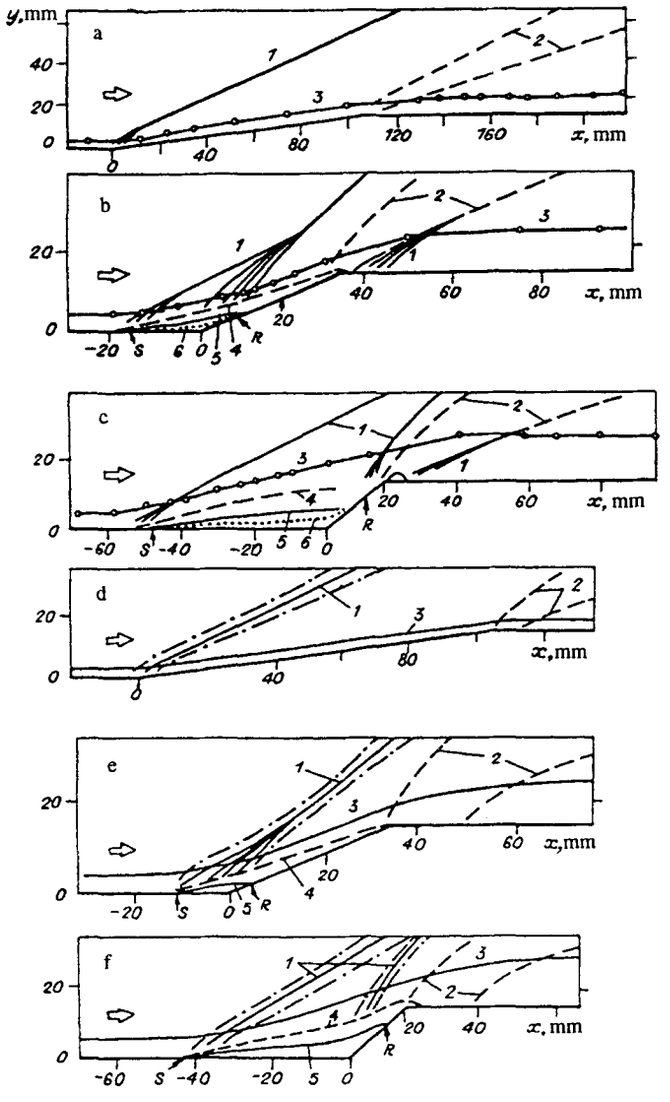

Fig. 1

The application of the parabolized equations demonstrated the possibility of predicting pressure distributions and velocity profiles for a continuous flow past steps and ledges with small slopes of up- and downwind sides. The above-mentioned computations on the basis of the complete equations show the possibility of satisfactory prediction of gas dynamics, pressure and friction distributions, and boundary-layer characteristics when separation zones localized at compression corners exist. At the same time it was shown that the heat transfer predictions fitted the experiments for the most part qualitatively, while the choice of an effective turbulence model depended on a sequence of shock and expansion waves [10]. The marked effect of a computational grid on the prediction of separation scales in a flow downstream of an oblique ledge was demonstrated [31].

The present work is a result of joint investigations performed at the Institute of Theoretical and Applied Mechanics (ITAM), Russian Academy of Sciences, Siberian Branch, and Rutgers University (USA) under a program of international scientific cooperation. It is devoted to a numerical study of successive interaction of the turbulent boundary layer with shock and expansion waves in a flow past oblique steps. The experimental data [22-25], which are also presented partly in [32], are used as a basis for testing the computations. The experiments were carried out under near-adiabatic-model-surface conditions in the T-313 supersonic wind tunnel with a working section measuring 0.6 by 0.6 m at ITAM. The configuration under investigation was a two-dimensional fixed-height (h = 15 mm) step with upwind-side slopes β = 8°, 25°, and 45°. A sufficiently large relative width of the model (b/h = 26.7) ruled out the effect of spatial end phenomena on the flow characteristics in the vicinity of the plane of symmetry. A developed turbulent boundary layer formed on the horizontal surface

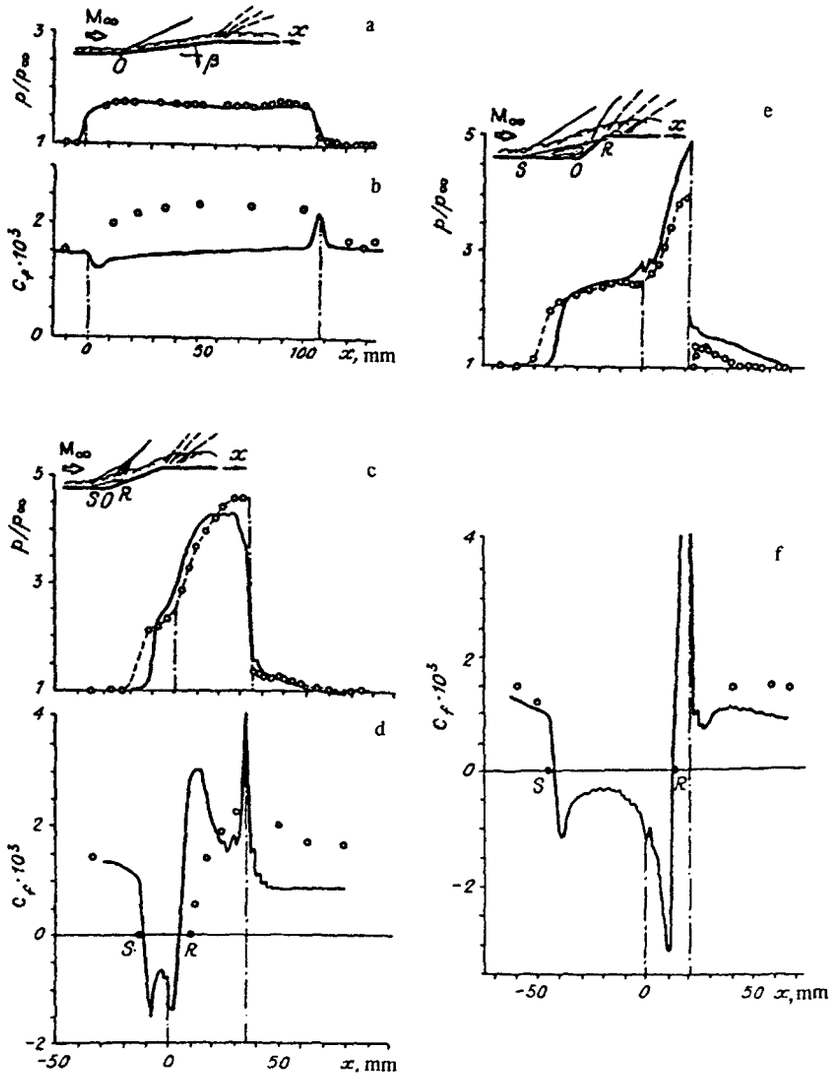

Fig. 2

upstream of the step. The layer, plug flow, and momentum thicknesses, δ, δ^*, and δ^{**}, respectively, before the steps are tabulated together with the main flow parameters for which detailed pneumometric sounding of the flow was carried out (p_0 and T_0 are deceleration temperature and pressure, and Re_1 is the unit Reynolds number).

Fields of total and static pressure in the vertical plane of model symmetry were measured by corresponding microsondes. Their orientation with allowance for expected washes ensured a total-pressure measurement error less than 1% and static, within 5%. Surface pressure distributions were measured along the line of model symmetry with an accuracy of 0.5% or better. The velocity was calculated from the pressure fields measured in the boundary layer according to the generalized Crocco integral. To determine the skin-friction coefficient from the total velocity profiles, we employed the procedure of [33], which was derived from the Ludwieg–Tillmann relationship generalized for compressible flows. This quantity was measured to accuracy about 10%, except in the regions of strong pressure gradients where the accuracy decreases to 15%. The flows were visualized by the Töpler and oil-black coating methods. The experimental conditions and procedures are described in greater detail in [22-25].

The computations were carried out at Rutgers University on the basis of the numerical solution to the averaged according to Favre nonstationary Navier–Stokes equations for a two-dimensional flow with the use of the algorithm and program developed at ITAM. We applied the absolutely stable implicit scheme of decomposing a stabilizing operator according

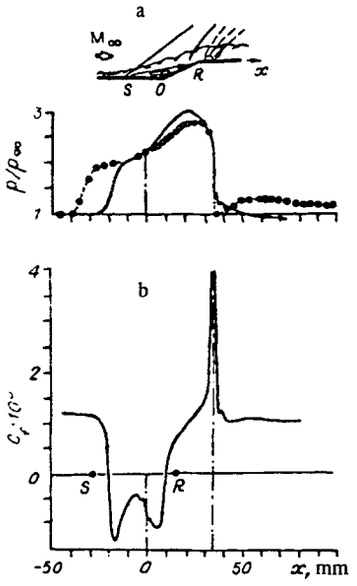

Fig. 3

to physical processes and along spatial directions [34, 35] to numerical integration of the equations. An asymmetric approximation of upstream convection and downstream pressure terms was defined on the explicit layer [36] in the form

$$L(uf)_i = \frac{\left((uf)_{i+1} - (uf)_{i-1}\right) - \left((|u|f)_{i+1} - 2(|u|f)_i + (|u|f)_{i-1}\right) - S_i}{2h},$$

$$S_i = \frac{1-\lambda}{2}\left((\overline{\delta f})^-_{i+\frac{3}{2}} - (\overline{\delta f})^-_{i+\frac{1}{2}}\right) + \frac{1+\lambda}{2}\left((\overline{\overline{\delta f}})^-_{i+\frac{1}{2}} - (\overline{\overline{\delta f}})^-_{i-\frac{1}{2}}\right) -$$
$$- \frac{1-\lambda}{2}\left((\overline{\overline{\delta f}})^+_{i-\frac{1}{2}} - (\overline{\overline{\delta f}})^+_{i-\frac{3}{2}}\right) - \frac{1+\lambda}{2}\left((\overline{\delta f})^+_{i+\frac{1}{2}} - (\overline{\delta f})^+_{i-\frac{1}{2}}\right),$$

where

$$(\overline{\delta f})^{\pm}_{i+\frac{1}{2}} = \operatorname{minmod}\left[(\delta f)^{\pm}_{i+\frac{1}{2}},\ \chi(\delta f)^{\pm}_{i-\frac{1}{2}}\right];$$

$$(\overline{\overline{\delta f}})^{\pm}_{i-\frac{1}{2}} = \operatorname{minmod}\left[(\delta f)^{\pm}_{i-\frac{1}{2}},\ \chi(\delta f)^{\pm}_{i+\frac{1}{2}}\right];$$

$$(\delta f)^{\pm}_{i+\frac{1}{2}} = (u^{\pm}f)_{i+1} - (u^{\pm}f)_i; \quad u^+ = \frac{u+|u|}{2}; \quad u^- = \frac{u-|u|}{2};$$

minmod[a, b] = 0 for sign(a) sign(b) < 0;

minmod[a, b] = sign(a) min(|a|, |b|) for sign(a) sign(b) > 0.

To approximate the pressure terms of the $\partial p/\partial x$ type, the function sign(−u) was substituted for the velocity u in the difference operator L.

The operator L approximates the initial differential operator $\partial/\partial x$ on smooth monotonic functions with terms of the second and, for $\lambda = 1/3$, third order:

$$L(uf)_i = \left(\frac{\partial uf}{\partial x} + h^2\frac{\lambda - \frac{1}{3}}{4}\frac{\partial^3 uf}{\partial x^3} + O(h^3)\right)_i.$$

In the vicinities of extrema of the function f the operator L is transformed into directed differences accurate to the first order, which allows one to eliminate strong oscillations in the regions of strong gradients in numerical solution. The parameter χ

$$\left(1 \le \chi \le \frac{3-\lambda}{1-\lambda}\right)$$

regulates a degree of shock-wave "spreading" in the course of computation. The approach employed is similar to the TVD method for a scalar equation [37]. The computation scheme ensured the observance of the conservation laws with transition to a steady state for each cell and was implemented by scalar three-point runs.

To close the initial equations, the two-parameter turbulence model put forward by Coackley [15] was applied in the context of the eddy viscosity concept, in which a characteristic scale q of the turbulence velocity and a specific rate ω of dissipation of turbulent kinetic energy were used as additional parameters:

$$\frac{\partial \rho s_i}{\partial t} + \frac{\partial \rho u_j s_i}{\partial x_j} = \frac{\partial}{\partial x_j}\left(\mu + \frac{\mu_t}{\mathrm{Pr}_i}\right)\frac{\partial s_i}{\partial x_j} + H_i,$$

$$\mathrm{Pr}_1 = 1, \qquad \mathrm{Pr}_2 = 1{,}3, \qquad \mu_t = C_t F \frac{\rho q^2}{\omega}.$$

Here $s_1 = q$; $s_2 = \omega$; $x_1 = x$; $x_2 = y$; the source terms H_i have the form

$$H_1 = \left(C_1\left(C_t F \frac{S^2}{\omega^2} - \frac{2}{3}\frac{D}{\omega}\right) - C_2\right)\rho q\omega,$$

$$H_2 = \left(C_3\left(C_t \frac{S^2}{\omega^2} - \frac{2}{3}\frac{D}{\omega}\right) - C_4\right)\rho\omega^2,$$

where

$$C_1 = \frac{1}{2}; \qquad C_2 = \frac{1}{2}; \qquad C_3 = 0{,}405F + 0{,}045; \qquad C_4 = 0{,}92;$$

$$C_t = 0{,}09; \qquad F = 1 - \exp(-\alpha \mathrm{Re}_t) \quad (\alpha = 0{,}0018); \qquad \mathrm{Re}_t = \frac{\rho q^2}{\mu\omega};$$

D is a velocity divergence, and S^2 is a strain-rate tensor invariant.

The chosen computation model offers a number of advantages over the others. This is attributed to a new form of representing the terms which depend on the turbulent Reynolds number Re_t and predict flow behavior for its small values. The use of the parameter q instead of turbulent kinetic energy allowed the author of the model to eliminate the need to introduce a special dissipation term into H_1 to counterbalance molecular diffusion in the laminar sublayer. Moreover, the use of the coefficient C_3 in the form of a linear function of the damping factor F with allowance for the character of evolution of the parameter ω made it possible to maximize the simplicity of the model and the degree of its compatibility with numerical methods.

The computational grid employed was uniform lengthwise and had from 120 to 150 stations spaced at intervals from 0.18 to 0.37 δ (δ is the thickness of an undisturbed boundary layer) depending on the configuration under study. It contained 75-80 points along the vertical coordinate and thickened toward the body surface by the logarithmic law. The degree of thickness was chosen so that the minimum distance from the wall to the nearest point at the starting station corresponded to $y^+ = 2.0$-2.5 (y^+ is a law-of-the-wall variable).

The initial conditions were determined by the uniform outer flow and the profile of a developed turbulent boundary layer at the station which was offset at least by five thicknesses of the undisturbed boundary layer from the zone of its interaction with a shock wave. The starting profile was defined on the basis of an exponential law of mean-velocity distribution with power 1/7, the generalized Crocco integral, and the ideal gas law for temperature and density. Near the body surface the mean-velocity profile was corrected so that the skin-friction coefficient was equal to the value found experimentally. To define

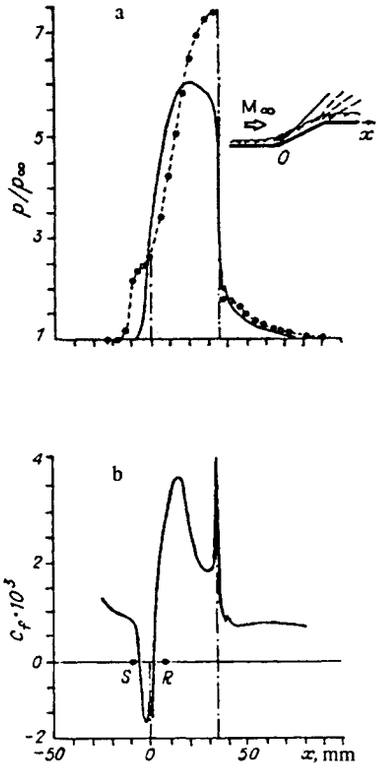

Fig. 4

the turbulent viscosity μ_t at the starting station, the two-layer algebraic model of Cebeci and Smith was used; the computation of the additional turbulence parameters was performed according to the relationships [38]

$$l = \sqrt{\alpha^*}\min(l_m, C_l\delta), \qquad q = \frac{\mu_t}{\rho l}, \qquad \omega = \frac{q}{l},$$

where $\alpha^* = 0.3$; l_m = kyF is the Prandtl displacement path length multiplied by the Van Driest damping factor (F = 1 — $\exp(-y^+/A^+)$, $A^+ = 26$); y is the distance to the wall; k = 0.41 is Karman's constant. Adhesion conditions, equality to zero of the characteristic turbulence-velocity scale q = 0, and the condition $\partial\omega/\partial y = 0$ were set at the wall, which was assumed to be adiabatic ($\partial T/\partial y = 0$).

In computations the adiabat exponent was taken equal to 1.405, the Prandtl number to 0.723, and the turbulent Prandtl number to 0.9. To define molecular viscosity, an exponent law with power 0.76 was used.

Joint analysis of experimental and calculated data for the fixed Mach number $M_\infty = 2.9$ with increasing slope of the oblique step side allows us to characterize the properties of the interaction of expansion and shock waves with the boundary layer under continuous and separated flows. Figure 1a-c presents the gas-dynamical flow diagrams obtained experimentally [22, 23] by detailed pneumometric sounding and optical visualization for obstacles with angles $\beta = 8°$, 25°, and 45°. The corresponding diagrams based on computations are shown in Fig. 1d-f.

A continuous flow past an obstacle is implemented in the case of small angles of flow deviation (Fig. 1a, $\beta = 8°$) for $M_\infty = 2.9$. Compression waves and a shock in the vicinity of the vertex of the compression corner are shown as lines 1; the positions of the first and last characteristics of a fan of expansion waves, as lines 2. Velocity profiles were measured at the stations which correspond to the circles along the outer edge of the boundary layer (lines 3). This edge was determined by the value of the relative velocity $u/u_e = 0.99$, where u_e is the local velocity of the outer flow. The corresponding calculated diagram of the flow is presented in Fig. 1d. The computation is seen to predict the main properties of such a flow. At the same time the effect of scheme viscosity leads to shock-wave "smearing." The boundaries of the "smearing" area are shown in the figure as dot—dash lines.

Increasing the compression angle up to $\beta = 25°$ (Fig. 1b) leads to formation of a separation zone between the flow-down (S) and spreading (R) lines, which were detected by oil-black visualization of limiting flow lines. The shock wave is transformed into the λ wave configuration over the separation zone. In so doing, a separated shock wave is generated in the vicinity of the line S, while a set of compression waves is generated over the line R. It should be noted that a homogeneous ideal-gas flow about such a configuration corresponds to existence of the oblique shock wave attached to the vertex of the compression corner. The M = 1, zero-velocity (u = 0), and maximum-reverse-flow-velocity (u_{rm}) lines 4-6 shown in the diagram characterize additional properties of the flow in the separation zone. A set of compression waves was discovered immediately behind the expansion waves in the flow past the step top. The diagram obtained by computation is also characterized by the existence of a separation zone at the compression corner (Fig. 1e). However, the zone is somewhat shorter than in the experiment, and there is still no distinct evidence of the λ wave configuration over it. The line of the maximum velocity of reverse flow is substantially closer to the surface (virtually coinciding with it in the figure) in comparison with the experiment. In addition, more significant decentering of the fan of expansion waves in the vicinity of the step vertex and no evidence of compression waves behind them are observed in the computations.

As the experiment shows (Fig. 1c), a further increase of the side slope up to $\beta = 45°$ is accompanied by the development of a large-scale separation before the obstacle and a corresponding upstream shift of the line S and the separated shock. The reattachment line R approaches the step top, and the second distinct shock wave originates over it. The homogeneous ideal-gas flow past such a configuration corresponds to the existence of the sole curved shock separated from the compression-vertex. An additional local separation zone forms on the upper surface in a flow past the step top. Compression waves, merging with a shock wave, were detected in the region of the second reattachment of the flow downstream of the expansion-wave fan. The gas-dynamical diagram obtained by computation for the conditions in question (Fig. 1f) is close to the experimental one. As before, we emphasize only that the separation zone is somewhat shorter; within it the line u_{rm} almost coincides with the surface, and there is no evidence of compression waves or a shock downstream of the fan of expansion waves. The computations correct the position of the line M = 1 immediately before the step. Its experimental determination by pneumometric sounding was difficult. A subsonic area of substantial thickness, which is detected in the reattached boundary layer downstream of the line R, is responsible for the global subsonic character of the flow past the step top as distinct from the previous situation (Fig. 1b, e), which is confirmed below by analysis of the data on surface pressure distribution.

A comparison of the experimental and calculated data on pressure and skin-friction coefficient C_f distributions for the configurations considered above is shown for $M_\infty = 2.9$ in Fig. 2. For $\beta = 8°$, the calculated pressure distribution (Fig. 2a, solid line) is in good agreement with the experiment (circles). The current pressure is related everywhere to its characteristic value for an undisturbed flow over a plate upstream of the obstacle. At the same time, the computation underestimates the skin friction (Fig. 2b, similar symbol notation) between the compression corner and step vertices (x = 0-108 mm) as compared with the experiment.

For $\beta = 25°$ the pressure distribution computation is in sufficiently good agreement with the experiment (Fig. 2c). For the sake of clearness the experimental points are connected by a dash line. This situation is characterized by the beginning of formation of an isobaric area (a pressure "plateau"), which is observed in the separation zone ahead of the corner ($x < 0$) in both experiment and computation. At the same time, in the computation the point of origin of the pressure growth is closer to the obstacle, and the areas of pressure growth are characterized by higher gradients in comparison with the experiment. A severe monotonic decrease of pressure, which is attributed to the supersonic-flow acceleration in the fan of expansion waves, is observed experimentally downstream of the step vertex ($x > 35.5$ mm). In the computation the adverse pressure gradients in this region are less significant because of the above-noted additional decentering of the wave fan.

The data on skin friction, which correspond to the case under consideration, are for the most part in qualitative agreement with the experiment (Fig. 2d). The computation reveals a skin-friction reduction to zero in the vicinity of the separation S and reattachment R lines detected experimentally (solid circles). The area of negative values corresponds to a recirculation zone, where measurements by the procedure employed were difficult. Like pressure, the calculated friction distribution is characterized by a more significant gradient in the area between the line R and the first maximum. The computation reveals an extra maximum in the vicinity of the step vertex (x = 35.5 mm). Its existence calls for further experimental verification. The friction level on the upper surface ($x > 35.5$ mm) is noticeably lower than in experiment.

The computation of the pressure distribution for $\beta = 45°$ is also in rather good agreement with experiment (Fig. 2e) and is characterized by the existence of a significant favorable gradient in the vicinity of the separation line, an area of almost constant value (a "plateau") in the separation zone, and repeat growth of pressure on the upwind step side (x = 0-21.2 mm). It should be noted, however, that the interaction zone before the step is shorter, and the pressure level on its upwind side is

higher, in the computations. An abrupt pressure drop is observed experimentally immediately behind the step vertex ($x > 21.2$ mm). It is ascribed to the subsonic character of the flow past the step under subcritical-boundary-layer conditions. As the distance from the vertex increases, the pressure grows again and then decreases gradually to the level corresponding to an undisturbed flow upstream of the obstacle. Earlier, a similar pattern was discovered in a pressure distribution for right-angled ($\beta = 90°$) steps [39]. The characteristic minimum downstream of the vertex was not predicted, although satisfactory agreement with the experiment was achieved away from the step. The computations fail to reveal the development of the local separation zone immediately behind the vertex as well (Fig. 1f). These discrepancies are likely to be caused by both the potentialities of the turbulence model employed and the grid resolution, which is inadequate to describe the small-scale properties noted above.

The data on friction are compared for $\beta = 45°$ in Fig. 2f. As can be seen from the figure, the computation predicts correctly the qualitative character of the friction distribution and the change of the separation scales (the positions of the points S and R) with increasing β. Unfortunately, the lack of experimental data in the separation zone does not allow us to make a more comprehensive comparison. It is believed that the above-noted proximity of the calculated maximum-reverse-flow-velocity line to the surface may point to a more significant expected calculated skin friction in comparison with reality. The emergence of the minima of calculated skin friction in the vicinity of the separation and reattachment points and its high values downstream of the step vertex after the passage of the expansion waves have also attracted our attention. Verification of these properties requires more detailed experimental data on friction.

Figure 3 presents additional results for the 25° step for $M_\infty = 2.2$. It should be emphasized that as for $\beta = 45°$, $M_\infty = 2.9$, a homogeneous ideal-gas flow past such a configuration corresponds to the existence of a curved shock wave separated from the vertex of the compression corner. Under these conditions a large-scale separation zone forms before the obstacle, and the reattachment point R of the boundary layer approaches the step vertex (Fig. 3a, b). It is remarkable that all the pressure-distribution characteristics (Fig. 3a) that were described above and shown in Fig. 2e for $\beta = 45°$ were detected experimentally under the conditions being considered. As in the case mentioned above, the computation does not predict the pressure-distribution properties attributed to a subcritical-boundary-layer flow about the step top. The separation-zone length, which is underestimated in comparison with the experiment, is also noteworthy (Fig. 3b).

An increase of the Mach number to 3.85 with a fixed angle ($\beta = 25°$) leads to a situation corresponding to the oblique shock wave attached to the vertex of the compression corner in ideal-flow conditions. In this experiment the separation length ahead of the obstacle decreases, the reattachment point R moves away from the step top, and the characteristic nonmonotone pressure distribution on the upper surface disappears (Fig. 4a, b). The computation predicts the tendency for reduction of the separation length correctly (Fig. 4b). At the same time, the isobaric area forming before the corner is not seen in the pressure distribution (Fig. 4a), while the pressure maximum predicted in the vicinity of the corner vertex is underestimated by approximately 20%.

The investigations have demonstrated the possibility of computation of the successive interaction of the turbulent boundary layer with shock and expansion waves on the basis of the averaged Navier–Stokes equations and one of the well-known differential models of turbulence. The satisfactory prediction of the main gas-dynamical flow characteristics and pressure distributions in the vicinity of oblique steps under supersonic flow has been demonstrated. Nevertheless, reliable prediction of skin-friction distributions and formation of small-scale separation zones calls for further improvement of computation procedures. The necessity of obtaining more detailed experimental data on skin friction in separation zones for the purpose of further verification of the model considered here and other well-known models of turbulence is apparent.

We are grateful to Prof. D. Knight for his help in performing the computations and discussion of the results.

This work was supported by a grant from the Russian Foundation for Fundamental Research (Prospectus Code 93-013-17708).

REFERENCES

1. O. M. Belotserkovskii and Y. M. Davydov, A Large-Particle Method in Gas Dynamics [in Russian], Nauka, Moscow (1982).
2. S. M. Belotserkovskii et al., Mathematical Simulation of Plane-Parallel Separated Flow Past a Body [in Russian], Nauka, Moscow (1988).
3. G. I. Petrov, "A system of shock and expansion waves in flow past bodies of complex shapes," in: Aerohydromechanics and Space Research [in Russian], Nauka, Moscow (1985), pp. 32-35.

4. V. F. Kamenetskii and L. I. Turchak, "Supersonic inhomogeneous ideal-gas flow past a body," in: Applied Mathematics Communications [in Russian], Comp. Cent. USSR Acad. Sci., Moscow (1982).
5. I. A. Graur, T. G. Elizarova, and B. N. Chetverushkin, "Numerical simulation of turbulent flow past a right-angled step," Mathematical Simulation, **2**, No. 2, 31-44 (1990).
6. L. V. Gogish and G. Yu. Stepanov, Turbulent Separated Flows [in Russian], Nauka, Moscow (1979).
7. L. V. Gogish and G. Yu. Stepanov, Separated and Cavitational Flows [in Russian], Nauka, Moscow (1990).
8. A. A. Zheltovodov, E. G. Zaulichnyi, and V. M. Trofimov, "Development of models for computation of heat transfer under supersonic turbulent separated flows," Zh. Prikl. Mekh. Tekh. Fiz., No. 4, 96-104 (1990).
9. N. Narayanswami, D. Knight, S. M. Bogdonoff, and C. C. Horstman, "Interaction between crossing oblique shocks and a turbulent boundary layer," AIAA J., **30**, No. 8, 1945-1952 (1992).
10. A. A. Zheltovodov, A. V. Borisov, D. D. Knight, C. C. Horstman, and G. S. Settles, "The possibilities of numerical simulation of shock waves/boundary layer interaction in supersonic and hypersonic flows," in: International Conference on the Methods of Aerophysical Research, Novosibirsk (1992), Pt. 1, pp. 164-170.
11. D. D. Knight, C. C. Horstman, G. S. Settles, and A. A. Zheltovodov, "3-D shock wave–turbulent boundary layer interactions generated by a single fin," Preprint No. 1-93 [in Russian], Academy of Sciences, Siberian Division, Institute of Theoretical and Applied Mechanics, Novosibirsk (1986).
12. U. M. Kovenya and N. N. Yanenko, A Splitting Method in Gas-Dynamical Problems [in Russian], Nauka, Novosibirsk (1981).
13. J. G. Marvin, "Turbulence modeling for computational aerodynamics," AIAA J., **21**, No. 7, 941-955 (1983).
14. W. P. Jones and B. E. Launder, "The prediction laminarization with a two-equation model of turbulence," Int. J. Heat and Mass Transfer, **15**, 301-314 (1972).
15. T. J. Coackley, "Turbulence modeling methods for the compressible Navier–Stokes equations," AIAA paper No. 83-1693, N. Y. (1983).
16. D. C. Wilcox and M. M. Rubesin, "Progress in turbulence modeling for complex flow fields including the effects of compressibility," NASA TP, 1517 (1980).
17. C. C. Horstman, "Hypersonic shock-wave turbulent-boundary-layer interaction flows — experiment and computation," AIAA paper No. 91-1760, Honolulu, Hawaii (1991).
18. C. Ong and D. Knight, "Hybrid MacCormack and implicit Beam–Warming algorithms for supersonic compression corner," AIAA J., **25**, No. 3, 401-407 (1987).
19. M. Visbal and D. Knight, "The Baldwin–Lomax turbulence model for two-dimensional shock-wave/boundary-layer interactions," AIAA J., **22**, No. 7, 921-928 (1984).
20. C. C. Horstman, C. M. Hung, and G. S. Settles, et al., "Reynolds numbers effects on shock-wave turbulent-boundary-layer interactions — a comparison of numerical and experimental results," AIAA paper No. 77-42, N. Y. (1977).
21. A. A. Prikhod'ko, V. I. Zavelion, and O. B. Polevoi, "Finite-difference and finite-element algorithms for computation of aerohydrodynamics and heat transfer of viscous fluids and gases," Computation Techniques, **2**, No. 5, 169-178, Academy of Sciences, Siberian Division, Institute of Computation Techniques, Novosibirsk (1993).
22. A. A. Zheltovodov, E. Kh. Shilein, and V. N. Yakovlev, "Development of a turbulent boundary layer under mixed interaction with shock and expansion waves," Preprint No. 28-83 [in Russian], Academy of Sciences, Siberian Division, Institute of Theoretical and Applied Mechanics, Novosibirsk (1983).
23. A. A. Zheltovodov and V. N. Yakovlev, "Development stages, structure, and turbulence characteristics of compressible separated flows in the vicinity of two-dimensional obstacles," Preprint No. 27-86 [in Russian], Academy of Sciences, Siberian Division, Institute of Theoretical and Applied Mechanics, Novosibirsk (1986).
24. A. A. Zheltovodov, E. G. Zaulichnyi, V. M. Trofimov, and V. N. Yakovlev, "Investigation of heat transfer and turbulence in compressible separated flows," Preprint No. 22-87 [in Russian], Academy of Sciences, Siberian Division, Institute of Theoretical and Applied Mechanics, Novosibirsk (1987).
25. A. A. Zheltovodov, L. Ch.-Yu. Mekler, and E. Kh. Shilein, "Characteristics of separated-flow development at compression corners after expansion waves," Preprint No. 10-87 [in Russian], Academy of Sciences, Siberian Division, Institute of Theoretical and Applied Mechanics, Novosibirsk (1987).
26. O. B. Polevoi and A. A. Prikhod'ko, "Solution of steady-state two-dimensional equations for a viscous heat-conducting gas by a marching method of increased accuracy," in: Mathematical Simulation of Processes of Heat and Mass Transfer, Dnepropetrovsk State University, Dnepropetrovsk (1988), pp. 55-61.

27. A. V. Borisov and V. B. Karamyshev, "Numerical simulation of separated turbulent flows," Izv. Sib. Div. Akad. Nauk Ser. Tekh. Nauk, No. 1, 37-43 (1990).
28. A. V. Borisov, A. A. Zheltovodov, and V. B. Karamyshev, "Problems and possibilities of simulating supersonic turbulent separated flows," in: Problems of Simulation in Wind Tunnels: Proc. of International Seminar, Novosibirsk, 25-29 July, 1988, **1**, Novosibirsk (1989), pp. 63-74.
29. A. V. Borisov, A. A. Zheltovodov, V. M. Trofimov, et al., "Analysis of turbulent separated flows in the vicinity of two-dimensional obstacles under supersonic speed conditions," in: Separated Flows and Jets, IUTAM Symposium, Novosirbirsk, USSR, 1990, Springer-Verlag, Berlin–Heidelberg (1991), pp. 332-336.
30. A. A. Zheltovodov and C. C. Horstman, "Experimental and numerical investigation of 2-D expansion/shock wave–turbulent boundary layer interactions," Preprint No. 2-93 [in Russian], Academy of Sciences, Siberian Division, Institute of Theoretical and Applied Mechanics, Novosibirsk (1993).
31. A. A. Zheltovodov, E. Kh. Shilein, and C. C. Horstman, "Separation development in the interaction of a shock wave with the turbulent boundary layer disturbed by expansion waves," Zh. Prikl. Mekh. Tekh. Fiz., No. 3, 58-68 (1993).
32. G. S. Settles and L. J. Dodson, "Hypersonic shock/boundary-layer interaction database," in: Report PSU-ME-90/91-003, Dept. of Mech. Eng., Penn State Univ., University Park, Pennsylvania (1990), pp. 107-120.
33. M. A. Gol'dfel'd and Yu. A. Saren, "Approximate determination of skin friction from a velocity profile of a two-dimensional compressible turbulent boundary layer," in: 3rd All-Union School in Aerophysical Investigation Techniques, No. 2, Academy of Sciences, Siberian Division, Institute of Theoretical and Applied Mechanics, Novosibirsk (1983), pp. 129-132.
34. A. V. Borisov, "Numerical investigation of supersonic viscous flows," Preprint No. 10 [in Russian], Academy of Sciences, Siberian Division, Institute of Theoretical and Applied Mechanics, Novosibirsk (1980).
35. A. V. Borisov and V. B. Karamyshev, "A method for numerical investigation of turbulent separated flows," Preprint No. 9-88 [in Russian], Academy of Sciences, Siberian Division, Institute of Theoretical and Applied Mechanics, Novosibirsk (1988).
36. A. V. Borisov and V. B. Karamyshev, "On a higher-order scheme for solution of steady-state aerodynamic problems," Simulation in Mechanics, **4**, (21), No. 1, 88-92, Novosibirsk (1990).
37. S. R. Charkravarthy and S. Osher, "A new class of high accuracy TVD schemes for hyperbolic conservation laws," AIAA Paper No. 85-0363, N. Y. (1985).
38. T. L. Chambers and D. C. Wilcox, "Critical examination of two-equation models for turbulence closure models for boundary layers," AIAA J., **15**, No. 6, 68-77 (1977).
39. V. S. Dem'yanenko and A. A. Zheltovodov, "Experimental investigation of turbulent-boundary-layer separation in the vicinity of a step," Izv. Akad. Nauk, Mekh. Zhidk. Gaza, No. 5, 73-80 (1977).